

ISOPHOT OBSERVATIONS OF POST-AGB STARS: FOSSIL RECORDS OF MASS LOSS

A. K. Speck¹, M. Meixner¹, D. Fong¹, & T. Ueta¹

Astronomy Department, University of Illinois at Urbana/Champaign, 1002 W. Green Street, Urbana, IL 61801, USA

ABSTRACT

We present ISOPHOT observations of post-AGB objects. These show fossil record of AGB mass loss which allow observational tests of theoretical models for stellar evolution.

Key words: ISOPHOT – post-AGB – planetary nebulae – protoplanetary nebulae – circumstellar dust – mass loss

1. INTRODUCTION

In the late stages of evolution, intermediate mass ($0.8\text{--}8M_{\odot}$) stars follow a path on the H-R diagram up the asymptotic giant branch (AGB; Iben & Renzini 1983). On their ascent of the AGB, these stars suffer intensive mass loss which leads to the formation of a circumstellar dust shell. At the tip of the AGB the mass loss stops/decreases, and the dust shell begins to drift away from the star. At this point, these stars move to the blue side of the H-R diagram, through the horizontal post-AGB or protoplanetary nebula (PPN) branch, evolving towards the planetary nebula (PN) phase. This is shown schematically in Fig. 1. The mass lost by these stars goes on to enrich the interstellar medium (ISM). Therefore understanding mass loss from these stars is important for interstellar processes and galactic chemical enrichment. However, the mechanisms and details of the evolution and mass loss for intermediate mass stars are not well understood.

The circumstellar shells around post-AGB objects contain the fossil record of their mass loss. This is shown schematically in Fig. 2. The dust furthest from the central star (at R_{\max}) represents the oldest mass loss, while material closer to the stars represents more recent mass loss. The inner radius (R_{\min}) of the dust shell represents the end of heavy mass loss and the end of the AGB phase of the star's evolution. The dust in the circumstellar shell is heated both from the inside by the central star and from the outside by the interstellar radiation field (ISRF), so that the dust temperature decreases with distance from the central stars until it levels out at $\sim 20\text{--}50\text{K}$ at a radius of $\sim 1\text{pc}$ (Young, Phillips & Knapp 1993; Gillett et al. 1986).

Images of the dust around the well studied carbon star IRC+10216 (Mauron & Huggins 1999) show that AGB

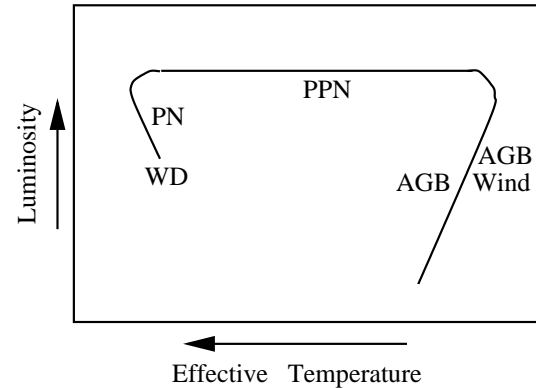


Figure 1. Schematic view of intermediate mass star evolution on the H-R diagram.

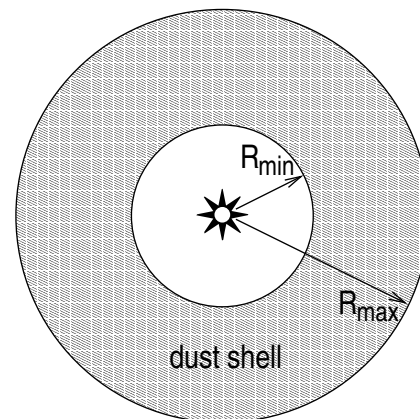


Figure 2. Schematic view of post-AGB star dust envelope.

stars have fairly spherically symmetric mass loss. This is further supported by the CO observations of TT Cyg (Olofsson et al. 2000). During the ascent of the AGB, the velocity of the outflowing mass appears to be fairly constant (e.g. Huggins, Olofsson & Johansson 1988). However, theoretical calculations suggest that the mass-loss rates should vary. Both Vassiliadis & Wood (1993) and Steffen, Szczerba & Schönberner (1998) have produced models of the evolution of those stars expected to evolve up the AGB including the effect of mass loss. Both groups suggested that the changes in surface luminosity of AGB stars as a result of the thermal pulse cycles should lead to variations in the mass-loss rate. In order to investigate

Table 1. Observations.

Source	Nebula Name	filters	phase
AFGL 2688	Egg	120, 180 μ m	PPN
AFGL 618	Westbrook	120, 180 μ m	PPN
HD161796		90, 160 μ m	PPN
NGC 246		90, 160 μ m	PN
NGC 6543	Cat's Eye	120, 180 μ m	PN
NGC 6720	Ring	90, 160 μ m	PN
NGC 6853	Dumbbell	90, 160 μ m	PN
NGC 7293	Helix	90, 160 μ m	PN

such variations, one needs to have an observable record of the AGB mass loss.

We are using ISOPHOT PHT 32 AOT observations of PPN and PN to investigate AGB mass loss recorded in the dust around such stars. We aim to answer some basic questions about the evolution of such stars:

What are the initial masses of stars which evolve into PNe?

What are the physical mechanisms for the mass loss experienced by these stars in their AGB phase?

2. OBSERVATIONS

We have obtained ISOPHOT PHT32 linear scans of the eight post-AGB objects, including three PPNe and 5 PNe, listed in Table 1. These linear scans, which are centered on the central star of the nebula, represent traverses across the entire circumstellar dust shells. The scans were imaged with two filters for each object. In most cases, we used the C100 90 μ m and C200 160 μ m filters, however in three cases, AFGL 618, NGC 6543 and AFGL 2688, we used the C200 120 μ m and 180 μ m filters because these sources are very bright and would saturate using the broader 90 and 160 μ m filters. The C100 90 μ m observations have 3 \times 3 pixel formats with 46'' pixel scale, while the C200 120 μ m, 160 μ m and 180 μ m observations have 2 \times 2 pixel formats with 92'' pixel scales. The PHT32 AOT uses a combination of raster mapping and chopper sweeping to create a map. For each raster step (of 60'' for the C100 and 92'' for the C200 filters), the chopper was used to make smaller steps of 15'' and 30'' to give an image pixel sizes of 15'' \times 46'' and 30'' \times 92'' for the C100 and C200 filters respectively. The linear scans used the maximum raster length possible of 30' and 46' for the C100 and C200 filters respectively. The chopper, however, sweeps across the raster position which increases the total length of the linear scans to 36' for the C100 and 53' for the C200 filters. Both forward and reverse scans were obtained in order to determine the repeatability of the observed structures. The ISOPHOT data presented in this paper was reduced using PIA (Gabriel et al. 1997).

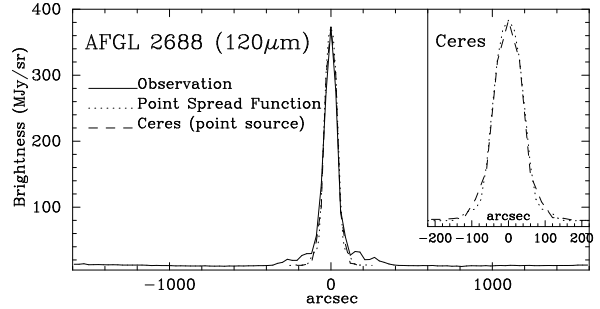


Figure 3. The profile of the 120 μ m linear scan of AFGL 2688 (solid line) together with the calculated PSF (dotted line) and the linear scan of Ceres (dashed), a point source.

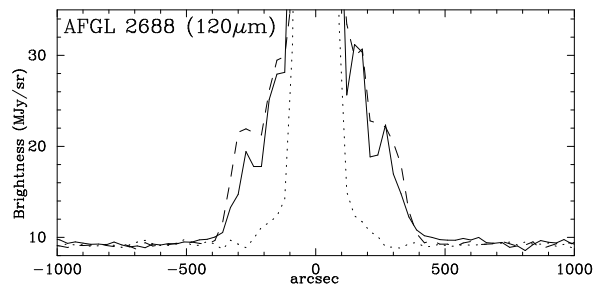


Figure 4. The profile of the 120 μ m linear scan of AFGL 2688: close up on extended emission. The solid line is the observation. The dotted line is a simulated point source of the same brightness. The dashed line is the simulated extended emission modeled using the PIA mapping simulator (see Speck et al. 2000).

3. PROTOPLANETARY NEBULAE

Fig. 3 shows the brightness profile of the ISOPHOT linear scan of the Egg at 120 μ m, comprising a bright point source surrounded by extended emission out to \sim 350''. The surface brightness of the extended emission is \sim 10% of the peak brightness of the point source. A closer look at the extended emission can be seen in Fig. 4, which shows that the distribution of the emission is not smooth, but rather shows periodic enhancements. Comparison of the 120 and 180 μ m scans (not shown), demonstrates their similar structure. The bumps in emission appear at the same radial distance at both wavelengths, showing that these bumps are not related to Airy rings.

Fig. 5 shows that the morphology of the thermal emission from AFGL 618 closely resembles that of AFGL 2688.

The positions of emission bumps represent enhanced mass loss. Using the distance to these objects and the outflow velocities (from the literature), we can find the spatial positions of the enhancements and the timescales for the enhanced mass loss. These are tabulated in Table 2.

The timescales for enhanced mass loss, in particular the time between successive pulses, compare favorably with predicted timescales of thermal pulses associated with the AGB phase and believed to affect mass loss (e.g Vassiliadis

Table 2.

Source	Distance (kpc)	v_{exp} (km/s)	R_{max} (")	R_{max} (kpc)	R_{inner} (")	R_{inner} (kpc)	R_{outer} (")	R_{outer} (kpc)	t_{max} (10^4 yrs)	t_{inner} (10^4 yrs)	t_{outer} (10^4 yrs)
AFGL 2688	1.2 ¹	22.4 ¹	350	~ 2	150	0.87	300	1.7	9	3.7	7.4
AFGL 618	1.7 ²	~ 20 ³	400	~ 3.3	160	1.3	275	2.3	16	6.4	11.7

1 - from Skinner et al. (1997); 2 - from Westbrook et al. (1975); 3 - from Meixner et al. (1998); v_{exp} = outflow velocity; R_{inner} = radius of enhanced emission closest to the central star; R_{outer} = radius of enhanced emission furthest from the central star; t_{max} = time since oldest part of the observable dust shell was ejected from the star; t_{inner} = time since enhanced emission closest to the central star was ejected from the star; t_{outer} = time since enhanced emission furthest from the central star was ejected from the star

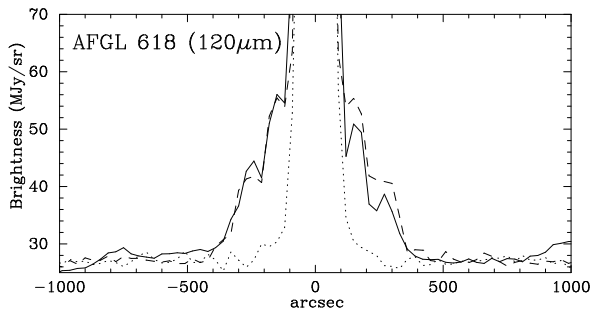


Figure 5. Same as Fig. 4 except for AFGL 618.

& Wood 1993; Steffen, Szczerba & Schönberner 1998). For a more detailed discussion of the relationship between the bumps in the dust shells and theoretical timescales for thermal pulses see Speck, Meixner & Knapp (2000). They found that the time between thermal pulses, as indicated by the spacing of the emission enhancements, was suggestive of progenitor masses for these carbon-rich PPNe of $\sim 3M_{\odot}$. It is interesting to note that the two PPNe which show the mass-loss enhancements (AFGL 2688 and AFGL 618) are both C-rich. PHT32 observations of the oxygen-rich PPN, HD 161796, shows a similarly large dust shell, but with much weaker emission and without any evidence for mass-loss modulation (Speck, Meixner & Ueta 2001). The factors affecting the occurrence of observable mass-loss modulations need further investigation.

4. PLANETARY NEBULAE

As a post-AGB object evolves further the central remnant star contracts and heats up. Once the stellar temperature is high enough to ionize the surrounding medium the object becomes a PN. At this stage the object becomes much more complex. A PN can be considered to be made up of concentric shells in which the level of ionisation decreases with distance from the central star. Therefore, close to the star the environment is characterized by highly ionized species, while the outer part of the nebula, not yet ionized is characterized by molecules and dust. This is shown schematically in Fig. 6. This complex structure makes the analysis of the ISOPHOT far-infrared (FIR) images much more complicated. For AGB stars and PPNe all the FIR

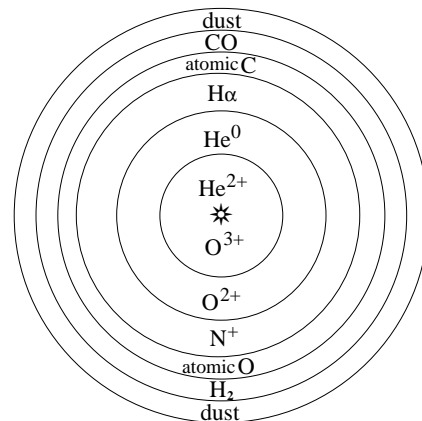
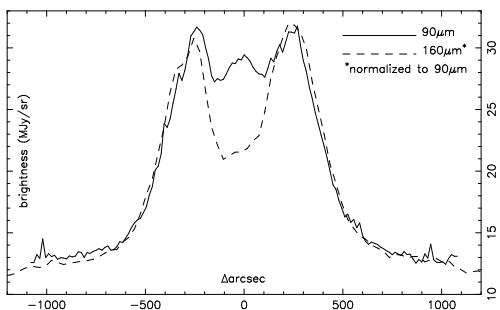


Figure 6. Schematic view of the structure of a planetary nebula.

Figure 7. The profile of the 90 μm and 160 μm linear scans of the Helix.

emission comes from cool dust, whereas for PNe there are also contributions from the FIR fine-structure lines of atomic and ionized species. The relative contributions from these species needs to be established before analysis of the dust distribution is possible.

One of the PNe in our sample, NGC 7293 (the Helix Nebula), is one of our nearest PNe at a distance of $\sim 200 \pm 50$ pc (Harris et al. 1996; Harrington & Dahn 1980). Its proximity gives the Helix a large angular size on the sky, making it extremely valuable for the study of the spatial distributions of different species in the nebula.

Fig. 7 shows the profiles of the linear scans of the Helix. In this case the 160 μm scan has been normalized to the 90 μm scan in order to demonstrate the differences in

morphology between the scans at these two wavelengths. These differences are clear in Fig. 7. The $90\mu\text{m}$ scan shows extra emission in the central region, not seen in the $160\mu\text{m}$ scan. The wavelength range of the $90\mu\text{m}$ filter includes the [O III] $88\mu\text{m}$ fine-structure line, while the wavelength range of the $160\mu\text{m}$ filter includes the [C II] $158\mu\text{m}$ fine-structure line.

In order to assess the relative contributions to the ISOPHOT broad bands from the ionized emission lines and from the dust continuum we have investigated the ISO LWS01 full grating observation ($43\text{--}196\mu\text{m}$) available from the ISO data archive (PI: Cox). We found that the [O III] $88\mu\text{m}$ line contributes less than $\sim 10\%$ of the flux in the $90\mu\text{m}$ band. For the $160\mu\text{m}$ band we can only obtain a rough estimate, since the LWS spectrum only goes to $196\mu\text{m}$ while the $160\mu\text{m}$ filter goes out to nearly $220\mu\text{m}$. However, we still find that the [C II] $158\mu\text{m}$ emission line contributes $\lesssim 20\%$ to the emission in this band, and probably more like 10% . In this way, we concur with Leene & Pottasch (1987) that the ionized emission lines do not contribute significantly to the emission in these broad FIR bands, with the majority of emission in our observations coming from cool dust. The LWS spectra were taken at the position of the optical ring of the Helix and not of the central cavity, therefore these estimates only hold for the ring region.

Let us assume that for the $160\mu\text{m}$ scan there is negligible contribution from the [C II] $158\mu\text{m}$ emission line, so that all the emission is from dust. Let us also assume that where this dust is present, as indicated by the $160\mu\text{m}$ scan, it is also the major contributor to the flux in the $90\mu\text{m}$ band. Therefore the excess emission in the central region of $90\mu\text{m}$ scan is not from dust. The only major atomic/ionized emission line that falls within the wavelength range of $90\mu\text{m}$ filter is the [O III] $88\mu\text{m}$. Therefore, we are seeing emission from [O III] in the central cavity of the Helix.

Therefore we believe that while most of the emission in the ISOPHOT observations of the Helix comes from cool dust around the nebula, there is a large contribution to the flux in the central region from [O III]. Speck, Meixner & Fong (2001) suggest that this is evidence for optically thick globules, analogous to the cometary knots (e.g. O'Dell & Handron 1996), in the central cavity of the Helix nebula. This work also shows the importance of accounting for the FIR emission lines when analyzing the ISOPHOT broadband observations.

Another result from the ISOPHOT data for the Helix nebula is that the dust shell is huge. There is low-level dust emission out to a radius of $\sim 1100''$. This is also seen in the FIR IRAS data. At a distance of 200pc , this equates to a radius of about 1pc , implying that there is a large mass of dust associated with the Helix (see Speck et al. 2001 for details).

5. CONCLUSIONS

We have shown that the ISOPHOT linear scans of PPNe and PNe provide unique information on their extended emission. For the C-rich PPNe, we have shown that they have large ($2\text{--}3\text{pc}$) dust shells which show evidence for mass-loss modulations due to thermal pulses. There seems to be a difference between the C-rich and O-rich PPNe in this respect. The only O-rich PPN to be studied thus far does not show any evidence for mass-loss modulations. For the PNe, we have only investigated the closest example, the Helix. We have shown that it is necessary to establish the relative contributions from cool dust and atomic/ionized lines to the FIR flux when using these observations. However, it is already clear that a massive dust shell is associated with the Helix nebula.

ACKNOWLEDGEMENTS

We are very grateful for help with data reduction from the ISOPHOT team at the ISO Data Centre (Carlos Gabriel, Rene Laureijs, Sybille Peschke and Bernard Schulz) and IPAC. We would also like to thank Mike Barlow and Jill Knapp for constructive conversations and correspondence. This work has been supported by NASA (JPL 961504 and STI 7898.02-96A). Meixner has also been supported by NSF (AST 97-333697).

REFERENCES

- Gabriel, C., et al. 1997, in ASP Conf. Ser. Vol. 125, *Astronomical Data Analysis Software and Systems VI*, ed. G. Hunt & H.E. Payne, (San Francisco: ASP), 108
- Gillett, F.C., Backman, D.E., Beichman, C., Neugebauer, G., 1986, *ApJ*, 310, 842.
- Harrington, R.S, Dahn, C.C, 1980, *AJ*, 85, 454.
- Harris, H.C., Dahn, C.C., Monet, D.G., Pier, J.R., 1996 in *IAU Symp. 180, Planetary Nebula*, H.J. Habing & Lamers, H.J.G.L.M. (eds), 40.
- Huggins, P.J., Olofsson, H., Johansson, L.E.B., 1988, *ApJ*, 332, 1009.
- Iben, I. Jr., Renzini, A. 1983, *ARAA*, 21, 271.
- Leene, A., Pottasch, S.R., 1987, *A&A*, 173, 145.
- Mauron, N., Huggins, P.J., 1999, *A&A*, 349, 203.
- Meixner, M., Campbell, M.T., Welch, W.J., Likkell, L., 1998, *ApJ*, 509, 392.
- O'Dell, C.R., Handron, K.D., 1996, *AJ*, 111, 1630.
- Olofsson, H., Bergman, P., Lucas, R., Eriksson, K., Gustafsson, B., Bieging, J.H., 2000, *A&A*, 353, 583.
- Skinner, C.J. et al. 1997, *A&A*, 328, 290.
- Speck, A.K., Meixner, M., Knapp, G.R., 2000, *ApJ*, 545, L145.
- Speck, A.K., Meixner, M., Ueta, D., 2001, in "Post-AGB objects (protoplanetary nebulae) as a phase of stellar evolution", Eds. S.K. Gorny, R. Szczerba, in press.
- Speck, A.K., Meixner, M., Fong, D., 2001, in review.
- Speck, A.K., et al., 2001, in preparation.
- Steffen, M., Szczerba, R., Schönberner, D., 1998, *A&A*, 337, 149.
- Vassiliadis, E., Wood, P.R., 1993, *ApJ*, 413, 641.
- Westbrook, W.E. et al. 1975, *ApJ*, 202, 407.
- Young, K., Phillips, T.G., Knapp, G.R. 1993, *ApJ*, 409, 725